Neuron
Article

Human Posterior Parietal Cortex Flexibly Determines Reference Frames for Reaching Based on Sensory Context

Pierre-Michel Bernier[1] and Scott T. Grafton[1,*]
[1]Department of Psychology, Brain Imaging Center, University of California, Santa Barbara, Santa Barbara, CA 93106, USA
*Correspondence: grafton@psych.ucsb.edu
DOI 10.1016/j.neuron.2010.11.002

SUMMARY

Current models of sensorimotor transformations emphasize the dominant role of gaze-centered representations for reach planning in the posterior parietal cortex (PPC). Here we exploit fMRI repetition suppression to test whether the sensory modality of a target determines the reference frame used to define the motor goal in the PPC and premotor cortex. We show that when targets are defined visually, the anterior precuneus selectively encodes the motor goal in gaze-centered coordinates, whereas the parieto-occipital junction, Brodman Area 5 (BA 5), and PMd use a mixed gaze- and body-centered representation. In contrast, when targets are defined by unseen proprioceptive cues, activity in these areas switches to represent the motor goal predominantly in body-centered coordinates. These results support computational models arguing for flexibility in reference frames for action according to sensory context. Critically, they provide neuroanatomical evidence that flexibility is achieved by exploiting a multiplicity of reference frames that can be expressed within individual areas.

INTRODUCTION

The planning of arm-reaching movements is achieved through a cascade of sensorimotor processes, from localizing a spatial goal to generating motor commands to move the limb. Complexity arises because the motor goal can be described at various levels of abstraction, either in terms of a hand displacement in space or in terms of a change in joint posture necessary to achieve it. Movement planning thus entails performing coordinate transformations in order to represent the motor goal in multiple reference frames (Battaglia-Mayer et al., 2003; Beurze et al., 2010; Chang and Snyder, 2010; Marzocchi et al., 2008; McGuire and Sabes, 2009; Medendorp et al., 2008; Pesaran et al., 2006; Pouget and Snyder, 2000). A long-lasting challenge has been to determine where these extrinsic and intrinsic representations are functionally nested in the brain.

Electrophysiological recordings in monkeys indicate that the posterior parietal cortex (PPC) constitutes a critical platform in which goal-directed actions are computed. The PPC contains a mosaic of sensorimotor regions each specialized in representing target locations for different effectors (Andersen and Buneo, 2002; Graziano and Gross, 1998). A set of areas in the dorsocaudal PPC, comprising the medial intraparietal area (MIP) and area V6A, are thought to be specifically involved in the planning of arm reaching movements (Andersen and Buneo, 2002; Galletti et al., 1997). A majority of neurons in these areas are selectively active during an instructed-delay period for intended arm movements, but not for eye movements (Snyder et al., 1997). Collectively, this general region of parietal cortex with selectivity for limb movements has been referred to as the "parietal reach region" (or PRR) (Andersen and Buneo, 2002; Snyder et al., 1997). A defining feature of neuronal activity in this region is that it tends to best describe the direction of an impending arm movement with respect to gaze (Batista et al., 1999; Buneo et al., 2002; Pesaran et al., 2006). Even reaches to nonvisual auditory targets are predominantly represented in a gaze-centered reference frame in this region (Cohen and Andersen, 2000). Together, these findings have formed the underlying basis of influential models of sensorimotor transformations arguing for a key role of the dorsocaudal PPC in providing an early high-level description of the motor goal in extrinsic visual coordinates, which would be converted into intrinsic body-centered coordinates for motor commands to be generated (Batista et al., 1999; Cohen and Andersen, 2002; Johnson and Ferraina, 1996; Medendorp et al., 2008).

There is mounting evidence establishing plausible functional homologies between human and monkey PPC (Astafiev et al., 2003; Culham et al., 2006; Grefkes and Fink, 2005). For example, several neuroimaging studies have identified a region in the human dorsomedial PPC, comprising the precuneate cortex and the parieto-occipital junction (POJ), that is also more active during the premovement preparation period for arm movements than for saccades (Astafiev et al., 2003; Connolly et al., 2003; Fernandez-Ruiz et al., 2007; Filimon et al., 2009; Levy et al., 2007; Tosoni et al., 2008). Furthermore, analogous to what is observed in the monkey, neuronal activity in the human PPC represents and updates visual target locations primarily in gaze-centered coordinates (Medendorp et al., 2005; Medendorp et al., 2003; Sereno et al., 2001). For instance, reach-related activity in the precuneus remains topographically (controlaterally) tied to the retinal coordinates of a remembered visual goal rather than to the actual direction of the movement, when the two vectors are dissociated with reversing prisms (Fernandez-Ruiz et al., 2007). Similarly, the reach errors associated with optic

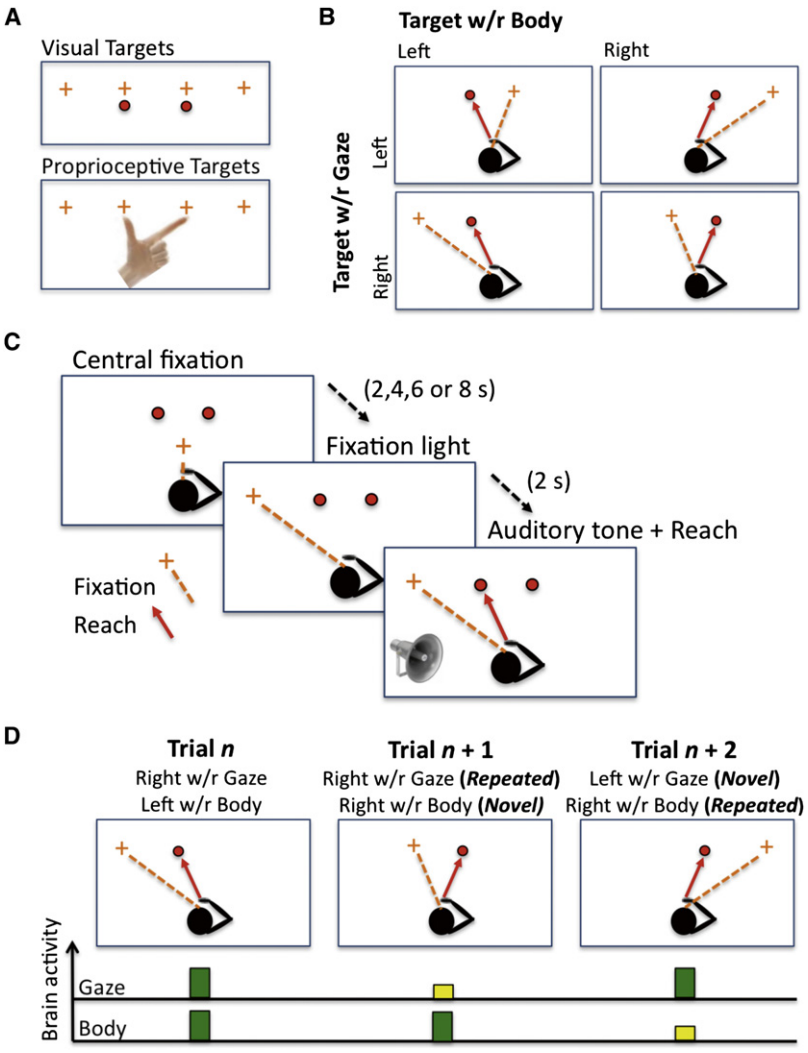

Figure 1. Task Structure and Trial Sequence

(A) On separate days, subjects reached toward two visual targets or two proprioceptive targets with their right index fingers. The visual targets consisted of red fiber optic endings, and the proprioceptive targets consisted of the thumb and index fingertips of the unseen left hand. The visual and proprioceptive targets were at the same spatial locations. Gaze was controlled by having subjects fixate at one of four peripheral fixation lights (orange crosses).

(B) Four target-gaze arrangements were used, such that on every trial, the target position could be defined as being either left or right with respect to body (body-centered reference frame) and left or right with respect to gaze (gaze-centered reference frame).

(C) Before every trial, subjects fixated on a central fixation light for 2, 4, 6, or 8 s. After this delay, one of the four peripheral fixation lights turned on, prompting subjects to direct their gaze to it. After a 2 s delay, an auditory tone served as a go signal by indicating which target to reach to. Subjects then initiated their reaching movement. Note that both visual targets remained lit during the entire duration of a trial. A single target is shown in (B) and (D) for the sake of clarity.

(D) A one-back repetition suppression (RS) paradigm was used with two factors (body-centered target position, gaze-centered target position) defined as being novel or repeated with respect to the previous trial. A reduced BOLD response for consecutive trials that are repeated along one of these factors is evidence that the identified voxel contains neurons that explicitly represent it (Desimone, 1996; Grill-Spector et al., 2006). For example, in trial n + 1, the gaze-centered target position (right) is repeated with respect to trial n, but the body-centered target position (right) is novel. Neural adaptation (i.e., lower BOLD response) is thus expected in brain regions that specifically encode the gaze-centered position of the target. Conversely, in trial n + 2, the gaze-centered target position (left) is novel with respect to trial n + 1, but the body-centered target position (right) is repeated. This trial would lead to lower BOLD response in brain areas that specifically encode the body-centered position of the target.

ataxia, a sensorimotor deficit arising from PPC lesions centered around the POJ (Karnath and Perenin, 2005), depend on a dynamic gaze-centered internal representation of remembered visual targets (Khan et al., 2005).

Despite considerable evidence for a predominant role of gaze-centered encoding for visual reaching in both monkey and human PPC, it remains to be shown whether a visual representation also holds when reach goals are defined solely by unseen proprioceptive signals, which are intrinsically encoded in body-centered coordinates (Lacquaniti et al., 1995). Recent computational models emphasize the flexibility with which the brain can weigh the extrinsic and intrinsic representations of the motor goal according to the available sensory input (McGuire and Sabes, 2009; Sober and Sabes, 2005), possibly being implemented at the single-cell level (Pouget and Snyder, 2000). In this light, we hypothesized that the reach-related regions of the human PPC might demonstrate a capacity to express different frames of reference as a function of target modality. We addressed this issue by manipulating the sensory nature of a target for reaching (visual or proprioceptive) while using fMRI repetition suppression to directly probe the reference frame in which the motor goal is defined (gaze- or body-centered) within a dorsal parietofrontal network.

RESULTS

Blood oxygen level-dependent (BOLD) signal was recorded while subjects reached toward two visual or two proprioceptive targets with their right index finger (Figure 1A). The visual and proprioceptive targets were at the same spatial locations, either left or right of the subjects' body midline. The fixation point was manipulated such that the targets could be located either left or right of the line of gaze. Thus, for each trial, the target position could be defined as being left or right in body-centered coordinates and left or right in gaze-centered coordinates (Figure 1B). The key manipulation was to tightly control the sequence of trials such that for every movement, the factors "Body-Centered Target Position" and "Gaze-Centered Target Position" could be either novel or repeated with respect to the preceding trial, according to a one-back repetition suppression (RS) design

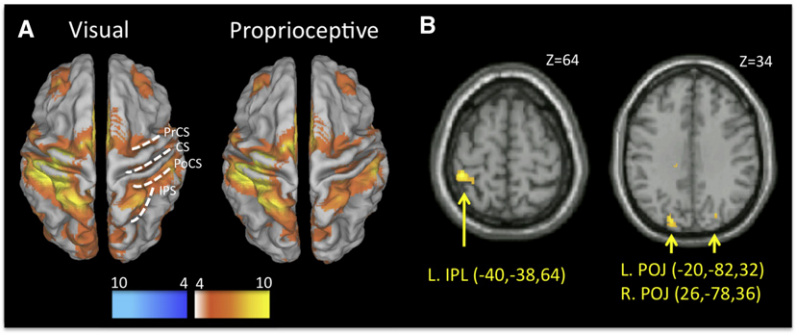

Figure 2. Reach-Related Activity Analysis

(A) Main effect of reaching in the visual and proprioceptive target conditions, overlaid on an inflated cortical surface. Both types of reaching incurred widespread activation in largely overlapping regions of the parietofrontal network. (B) Reaching to visual targets incurred greater activity in the left IPL, bilateral POJ, and bilateral extrastriate visual cortex (not shown) than proprioceptive targets. Coordinates (x, y, z) are expressed in the MNI system ($p < 0.001$). The following abbreviations are used: PrCS, precentral sulcus; CS, central sulcus; PoCS, postcentral sulcus; IPS, intraparietal sulcus.

(Figure 1D). By exploiting the habituation of neural responses to repeated experiences of a stimulus (Desimone, 1996; Grill-Spector et al., 2006), RS could be used to delineate the cortical areas that specifically encode the motor goal in body-centered and/or gaze-centered coordinates (see Van Pelt et al., 2010 for similar methodology for eye movements).

Reach-Related Activity Analysis

The first objective was to identify the brain areas specifically recruited for the planning of reaching movements to visual or proprioceptive targets. To do so, we contrasted activations obtained in a reach task to those obtained in a static task in which no reach was produced (reach > static; see Experimental Procedures). As seen in Figure 2A, a very similar set of reach-related regions was observed for visual and proprioceptive targets. Irrespective of the sensory modality of the target, the left motor cortex was activated, consistent with motion of the right hand. The parietal cortex was also activated bilaterally, including the postcentral sulcus, the superior parietal lobule (SPL), the inferior parietal lobule (IPL), the intraparietal sulcus (IPS), and the POJ. In the frontal lobe, the dorsal and ventral aspects of the premotor cortex (PMd and PMv respectively), as well as the middle frontal gyrus, were significantly recruited by both tasks. Overall, these activations are very consistent with those previously reported using similar contrasts (Astafiev et al., 2003; Filimon et al., 2009; Grafton et al., 1992; Prado et al., 2005). Comparisons across target modalities revealed negligible differences in reach-related activations. Reaching to visual targets incurred more activity in the left IPL, bilateral POJ, and bilateral extrastriate visual cortex than reaching to proprioceptive targets (Figure 2B). No region was found to be more active for reaching to proprioceptive targets than visual targets ($p < 0.001$).

Differential activations for each level (left, right) of the factor "Gaze-Centered Target Position" were then compared. As expected, in the visual target condition, the gaze-centered position of the target incurred significant contralateral activation in visual areas of the occipital lobe (see Figure S1 and Table S1 available online). Interestingly, two clusters in bilateral SPL, located slightly dorsal to the medial branch of the IPS, also showed contralateral topography for visual targets. These activations are consistent with an area in the medial end of the IPS previously reported to show contralateral preference for arm and eye movements (Medendorp et al., 2005; Medendorp et al., 2003) and retinotopic organization for memorized visual targets (Sereno et al., 2001). These contralateral activations indirectly confirm that subjects complied with the requirement not to break fixation during the task and produce the reaching movements with the target in peripheral vision (see Experimental Procedures). Neural activity for reaches to unseen proprioceptive targets also depended on the gaze-centered position of the target, but the pattern of activity differed fundamentally from that observed in the visual condition. Instead of contralateral recruitment, there was an increase in activity in bilateral IPS and premotor regions when proprioceptive targets were left of gaze, as compared to when they were right of gaze. No region showed more activity in the reverse contrast (right with respect to [w/r] gaze > left w/r gaze). This pattern of results strongly suggests that proprioceptive targets are represented differently in the parietofrontal network than visual targets.

The same analysis was performed for the two levels of the body-centered target position. Irrespective of target modality, reaching to the left target incurred significantly more activity in the SPL and sensorimotor regions bilaterally than reaching to the right target (Figure S1 and Table S2). This may be related to the greater computational/biomechanical demands associated with moving the right hand to the left as compared to the right (more degrees of freedom, greater inertia), because no region showed more activity for the reverse contrast (right w/r body > left w/r body).

Repetition Suppression Analysis

The main objective of the present experiment was to determine which of the reach-related regions explicitly represented the motor goal in gaze-centered and/or body-centered coordinates, as well as whether this pattern depended upon the sensory modality of the target. To do so, we assessed the repetition suppression effects for gaze and body by contrasting the novel trials with the repeated trials, done separately for each target modality. Importantly, these RS analyses were carried out using the reach-related regions identified in the preceding analysis as inclusive masks (set at $p < 0.001$; see Experimental Procedures), effectively eliminating brain regions solely associated with the planning of eye movements.

Visual Target Condition

In the visual target condition, several regions showed sensitivity to repetition suppression of either the gaze-centered or the body-centered target positions (Figure 3A; Table 1). The largest

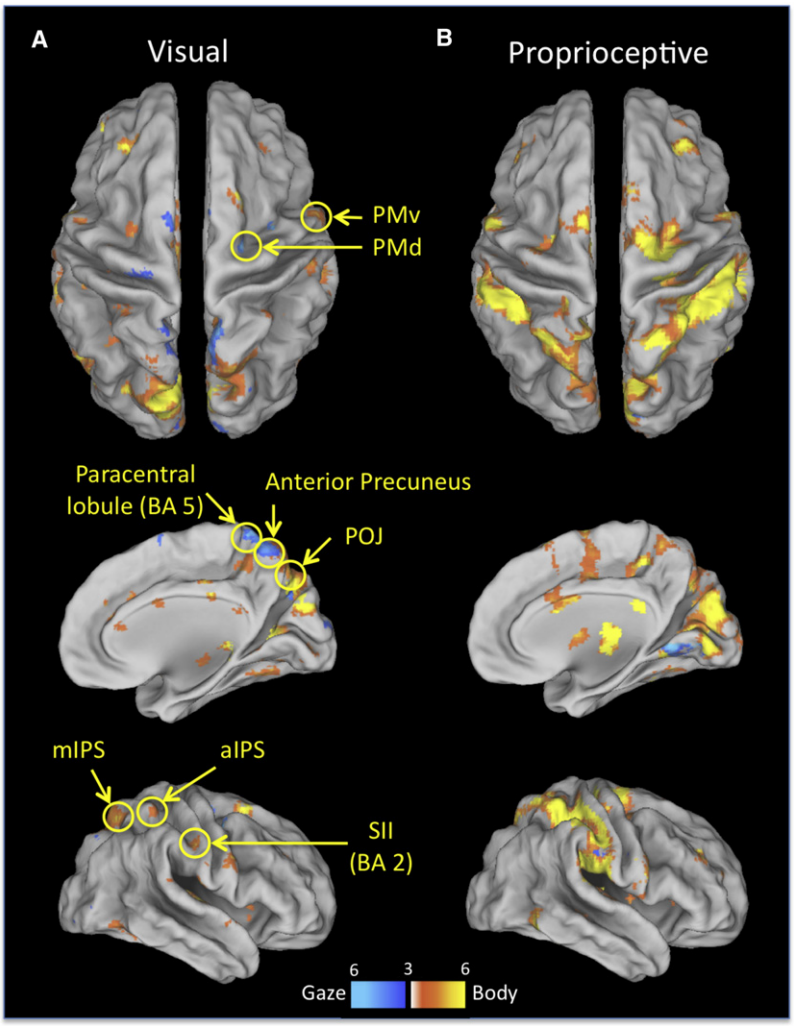

Figure 3. Repetition Suppression Analysis

(A and B) Areas showing significant suppression for repeated gaze-centered target positions (in blue) and repeated body-centered target positions (in red) in the visual (A) and proprioceptive (B) conditions ($p < 0.005$). The circles in (A) correspond to the approximate locations of the ROIs drawn around every region, showing significant repetition suppression for gaze or body in the visual target condition (only right hemisphere ROIs shown; see Table 1 for exact peak coordinates).

cluster showing RS for gaze was located in the anterior precuneus bilaterally, with local maxima at peak Montreal Neurological Institute (MNI) coordinates of (−8, −58, 60) and (4, −58, 64) for left and right hemispheres, respectively, corresponding to human cytoarchitectonic area 7A (Scheperjans et al., 2008a; Scheperjans et al., 2008b; Scheperjans et al., 2005; see Experimental Procedures). Interestingly, the anterior precuneus appeared to encode the motor goal selectively in visual coordinates, because we did not find significant RS for body anywhere along the medial SPL in the visual target condition. Consistent with recent work suggesting that a reach-selective cluster of activation in the precuneus encodes the spatial goal of the movement in retinal coordinates (Fernandez-Ruiz et al., 2007), the present selectivity for gaze-centered encoding in the anterior precuneus provides additional evidence that this region constitutes a key node in which visual reaching movements are represented in high-level extrinsic coordinates.

Several areas showed RS for both gaze- and body-centered target positions in the visual condition, suggesting a mixed representation. This was the case for BA 5 in the paracentral lobule (cytoarchitectonic area 5M), at locations slightly rostral to the anterior precuneus cluster, as well as in the PMd (junction of precentral sulcus and superior frontal sulcus). These findings are congruent with monkey neurophysiology and human neuroimaging studies, which report an encoding of the motor goal both in eye and hand coordinates in BA 5 (Buneo et al., 2002) and PMd (Batista et al., 2007; Beurze et al., 2010; Pesaran et al., 2006). RS effects also indicated a mixed representation in the POJ (cytoarchitectonic area 7M), although RS for body was predominant. Interestingly, the RS effects in these regions were lateralized to some extent, with clusters of RS for gaze being observed in the right hemisphere and RS for body being most prominent in the left hemisphere (see Table 1). This pattern of results supports the existence of a hemispheric asymmetry in coordinate representations for reaching (Pellijeff et al., 2006) and may explain why right PPC damage predominantly impairs reaching to visual targets (Jackson et al., 2000), whereas left PPC damage mainly impairs postural control (Sirigu et al., 1995).

In the visual target condition, selective RS for body-centered target positions was found in the rostral aspects of the parietal lobe, with maxima in the anterior part of the IPS bilaterally (aIPS; cytoarchitectonic area 7PC), as well as in the right postcentral sulcus, corresponding to BA 2. These rostral body-centered activations support the existence of a posteroanterior gradient of visual-to-somatic information in the parietal cortex, consistent with single-cell recordings in monkeys (Battaglia-Mayer et al., 2003). Significant RS for body was also found bilaterally in the middle section of the medial bank of the IPS, which we labeled mIPS (cytoarchitectonic area 7A). In the frontal lobe, significant clusters of RS for body were observed in bilateral PMv, in line with this region in the monkey also encoding visual targets for reaching in body-centered coordinates (Graziano et al., 1994).

Proprioceptive Target Condition

A very different pattern emerged in the proprioceptive target condition. There was negligible repetition suppression for gaze. Instead, there was robust RS for body across several

Table 1. Average Peak MNI Coordinates of Clusters Showing Significant Repetition Suppression for Gaze-Centered Target Position and Body-Centered Target Position in the Visual Condition

Anatomical Region	Functional Label (Brodman Area)	Hemisphere	x	y	z	t value
Gaze						
Precentral sulcus	PMd (BA 6)	Right	16	−10	60	4.72
Paracentral lobule	BA 5	Right	2	−46	68	4.30
Superior parietal lobule	Anterior precuneus (BA 7)	Left	−8	−58	60	3.04
		Right	4	−58	64	3.38
Parieto-occipital junction	POJ (BA 7, 19)	Right	20	−72	36	3.5
Body						
Frontal lobe	Middle frontal gyrus (BA 9)	Left	−24	44	36	4.41
		Right	34	38	30	3.32
Precentral sulcus	PMd (BA 6)	Left	−26	0	54	3.59
	PMv (BA 6)	Left	−50	−2	30	4.07
		Right	52	4	24	3.86
Postcentral sulcus	SII (BA 2)	Right	44	−32	42	3.64
Paracentral lobule	BA 5	Left	−10	−44	62	3.53
Intraparietal sulcus	aIPS (BA 7)	Left	−28	−52	48	3.46
		Right	44	−46	54	3.38
	mIPS (BA 7)	Left	−14	−62	56	3.87
		Right	14	−62	58	4.27
Parieto-occipital junction	POJ (BA 7, 19)	Left	−14	−84	38	5.39
		Right	16	−74	40	5.29

All activations are significant at $p < 0.005$ uncorrected; minimum cluster size 10 voxels. Values in x, y, and z are shown in mm.

parietal and premotor areas (Figure 3B and Table 2). All areas with some level of sensitivity to gaze for visual targets (anterior precuneus, POJ, BA 5, PMd) did not necessarily show RS for gaze in the proprioceptive condition, but actually reversed their mode of representation to show strong RS for body. Critically, there were significant clusters of RS for body in the left and right anterior precuneus, where RS for gaze was most prominent in the visual target condition. The peak coordinates were located at (−10, −54, 66) and (14, −56, 64) for left and right hemispheres, respectively (also corresponding to cytoarchitectonic area 7A). These peaks were slightly more dorsal and lateral than those in which RS for gaze was observed in the visual condition (~6 mm) but were still within the localization accuracy associated with the 8 mm smoothing kernel, suggesting considerable spatial overlap across target conditions. Clusters showing significant RS for body were also observed in bilateral POJ, BA 5, and PMd. The clusters in the right POJ, right BA 5, and right PMd were largely coextensive with those in which RS for gaze was observed in the visual target condition, with peak coordinates located in the same cytoarchitectonic areas (7M for the POJ and 5M for BA 5).

In addition to these reversals from a gaze- to a body-centered representation, proprioceptive reaching was associated with significant clusters of RS for body in rostral parts of the parietal lobe, especially in the postcentral sulcus (BA 2) and aIPS. Activation in BA 2 reached significant levels bilaterally in the proprioceptive condition, whereas it was only observed in the right hemisphere in the visual condition. A greater involvement of rostral parietal areas for proprioceptive targets is consistent with the finding that ablation of the anterior SPL in monkeys causes misreaching for proprioceptive targets in the dark but has less of a detrimental effect for visual targets in the light (Rushworth et al., 1997). Significant clusters of RS for body were also observed in other areas that showed RS for body in the visual target condition (mIPS, PMv).

The whole brain analysis did not reveal any area showing RS for gaze in the proprioceptive condition ($p < 0.005$). In an exploratory analysis, the statistical threshold was lowered to $p < 0.01$ to test for a more subtle RS effect for gaze (Figure S2). Interestingly, this analysis exposed only two clusters in the entire parietofrontal network, both located on the superior edge of the POJ bilaterally. The local maxima were at (−4, −78, 52) for the left hemisphere and at (20, −78, 48) and (4, −62, 62) for the right hemisphere (cytoarchitectonic area 7P). This analysis suggests that a fraction of neurons in the superior POJ may still use a visual code to represent unseen proprioceptive targets, perhaps subtending the small, yet significant, bias exerted by gaze direction on the accuracy of reaches directed toward unseen body parts (Pouget et al., 2002b).

Region of Interest Analysis

The main finding of the present study is the change in the representation of the motor goal in several regions of the parietofrontal network as a function of the sensory modality of the target. To quantitatively assess this relative change in sensitivity, we functionally defined 8 mm spherical regions of interest analysis (ROIs) around the peak of each area identified in the visual target condition (all regions listed in Table 1, except MFG) and then assessed

Table 2. Average Peak MNI Coordinates of Clusters Showing Significant Repetition Suppression for Body-Centered Target Position in the Proprioceptive Condition

Anatomical Region	Functional Label (Brodman Area)	Hemisphere	x	y	z	t value
Body						
Frontal lobe	Middle frontal gyrus (BA 9)	Right	36	44	30	3.94
Precentral sulcus	PMd (BA 6)	Left	−30	−12	58	3.40
		Right	22	−16	60	4.78
	PMv (BA 6)	Left	−54	0	32	5.59
		Right	56	6	32	3.64
Postcentral sulcus	SII (BA 2)	Left	−42	−32	42	8.69
		Right	48	−34	52	6.52
Paracentral lobule	BA 5	Left	−10	−46	62	4.09
		Right	12	−42	56	3.72
Intraparietal sulcus	aIPS (BA 7)	Left	−42	−42	52	6.35
		Right	34	−46	58	5.43
	mIPS (BA 7)	Left	−20	−62	62	3.79
		Right	20	−62	60	3.66
Superior parietal lobule	Anterior precuneus (BA 7)	Left	−10	−54	66	4.44
		Right	14	−56	64	4.16
Parieto-occipital junction	POJ (BA 7, 19)	Left	−14	−74	46	3.21
		Right	12	−72	42	3.07

All activations are significant at $p < 0.005$ uncorrected; minimum cluster size 10 voxels. Values in x, y, and z are shown in mm.

the extent of suppression for gaze and body in these ROIs in the proprioceptive target condition (see Experimental Procedures). Importantly, because ROIs were drawn around the same coordinates in the two target conditions, any change in sensitivity to gaze and body would arise from the same region of cortex and is therefore likely to be subtended by shared neuronal populations within the ROI.

These analyses confirmed the reversal in sensitivity within the anterior precuneus as a function of target modality, as shown in Figure 4. A two-way repeated-measures analysis of variance (ANOVA) revealed a significant interaction between the sensitivity of the anterior precuneus to gaze and body and the sensory modality of the target ($F_{(1,17)} = 6.54$; $p = 0.02$). Breakdown of this interaction with paired t tests revealed that in the visual condition, RS for gaze was significantly greater than RS for body ($p = 0.04$), but that in the proprioceptive condition, RS for body was significantly greater than RS for gaze ($p = 0.04$). These preferences for gaze or body were generally consistent across subjects, as can be seen in the scatter plots in Figure 4D. Fourteen out of 18 subjects showed more RS for gaze than body in the visual condition, and 14 subjects showed more RS for body than gaze in the proprioceptive condition. To further assess the local nature of the reversal in sensitivity in the anterior precuneus, we carried out the same statistical analysis with data extracted from smaller 5 mm ROIs drawn around the same peak coordinates (i.e., peak of RS for gaze in the visual condition). Even with this more conservative approach, the interaction was revealed to be significant ($F_{(1,17)} = 5.05$; $p = 0.04$). This confirms that the reversal in sensitivity was expressed within a very confined region of cortex in the anterior precuneus (within voxels that were actually most biased for gaze in the visual condition) and was not driven by voxels from a contiguous area expressing more body-centered encoding (e.g., BA 5).

The ROI analysis also revealed the pattern of RS characterizing a mixed representation in BA 5 and PMd (Figure 5). The extent of suppression to gaze and body in these areas was similar in the visual condition but became much greater for body than gaze in the proprioceptive condition. The ANOVA revealed a significant interaction in BA 5 ($F_{(1,17)} = 4.46$; $p = 0.04$), whereas a trend for an interaction was observed in PMd ($p = 0.14$). Paired t tests confirmed that RS for gaze and body did not differ in the visual condition ($p > 0.4$ in both regions), but that RS for body was significantly greater than RS for gaze in the proprioceptive condition ($p = 0.03$ in BA 5 and $p = 0.04$ in PMd). The ROI analysis also revealed a mixed pattern of sensitivity in the POJ ($p > 0.1$ in paired t tests between RS for gaze and RS for body; Figure 6). Still, this region was biased to representing the motor goal predominantly in body-centered coordinates for both target modalities, as reflected by the fact that the main effect of sensitivity almost reached significant levels ($p = 0.10$). Finally, the ROI analyses carried out on the areas in which significant clusters of RS for body were observed in both target conditions (i.e., aIPS, mIPS, PMv, and BA 2) revealed a significant main effect of sensitivity in each of them ($p = 0.03$ in aIPS, $p = 0.04$ in mIPS, $p = 0.01$ in PMv, $p = 0.01$ in BA 2). Paired t tests confirmed that RS for body was significantly greater than RS for gaze in these areas for both conditions ($p < 0.01$; see Figure S3), except for aIPS and mIPS in the visual condition ($p > 0.05$).

DISCUSSION

Evidence from monkey neurophysiology and human neuroimaging highlights the dominant nature of visual representations of

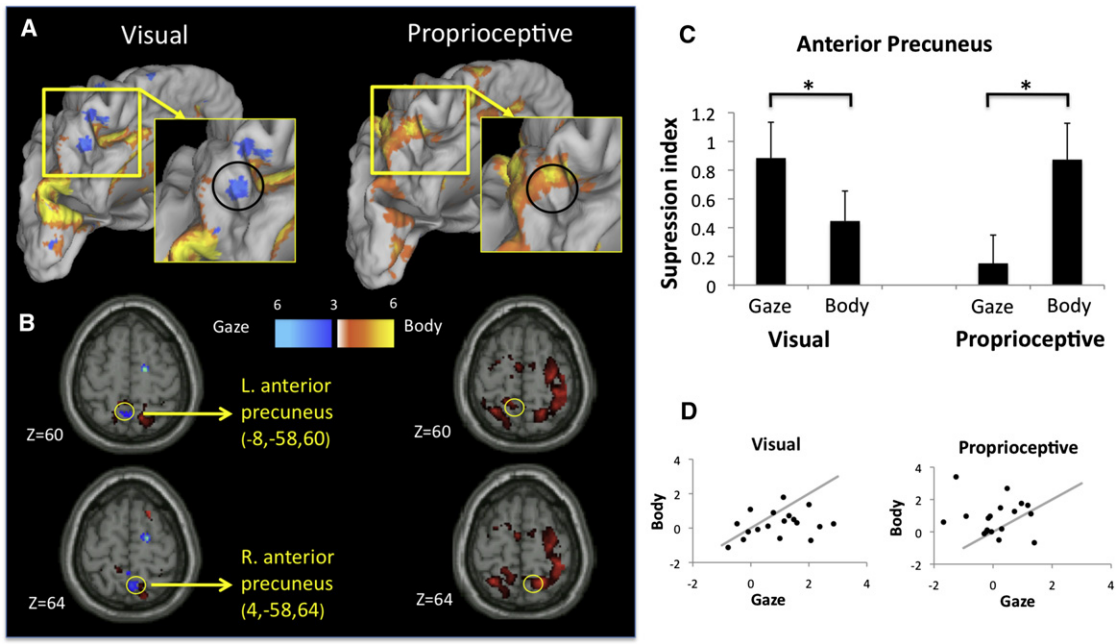

Figure 4. Reversal in Sensitivity to Gaze and Body as a Function of Target Modality in the Anterior Precuneus

(A) Posteromedial view of the left hemisphere with areas showing significant RS for gaze (in blue) and body (in red) in the visual and proprioceptive target conditions ($p < 0.005$). The approximate location of the anterior precuneus ROI is circled in the insets.

(B) Same activations overlaid on axial anatomical slices (ROIs circled).

(C) Suppression index for gaze and body in the visual and proprioceptive target conditions in the anterior precuneus (data collapsed across both hemispheres). Error bars represent standard error (SE). *$p < 0.05$.

(D) Scatter plots showing the same data (RS for body versus RS for gaze) for each subject. Most subjects showed greater sensitivity to gaze than body in the visual condition (data points below the diagonal) but greater sensitivity to body than gaze in the proprioceptive condition (data points above the diagonal).

the motor goal in the PPC (Andersen and Buneo, 2002; Batista et al., 1999; Buneo et al., 2002; Fernandez-Ruiz et al., 2007; Medendorp et al., 2008). Yet it is unknown whether the PPC also uses a visual code when movements are directed toward unseen proprioceptive target locations. We manipulated the sensory modality of a target for reaching and exploited fMRI repetition suppression to probe the reference frame in which the motor goal is represented in the PPC, as well as in connected premotor areas. The anterior precuneus was found to encode the motor goal for reaches to visual targets selectively in gaze-centered coordinates. Other areas of the parietal lobe (POJ, BA 5) and premotor cortex (PMd) showed a mixture of gaze- and body-centered encoding, providing evidence for a heterogeneity of representations for visual reaching in the human parietofrontal network (Battaglia-Mayer et al., 2003; Beurze et al., 2010; Chang and Snyder, 2010; Marzocchi et al., 2008; McGuire and Sabes, 2009; Medendorp et al., 2008; Pesaran et al., 2006; Pouget and Snyder, 2000). In stark contrast, reaching to proprioceptive targets was associated with negligible gaze-centered encoding but considerable body-centered encoding throughout the parietofrontal network. Remarkably, RS for body was evident in every region that showed some level of RS for gaze in the visual condition, including the anterior precuneus. These results argue for flexibility in reference frames for action according to sensory context (McGuire and Sabes, 2009; Sober and Sabes, 2005). Critically, they demonstrate that flexibility is not achieved by engaging different brain areas each using a fixed gaze- or body-centered reference frame, but by recruiting many of the same areas that themselves change their mode of representation.

The present reversal in motor goal representation provides empirical support for computational models, suggesting that the weighting of extrinsic and intrinsic representations of the motor goal is dictated by the sensory modality of the target (McGuire and Sabes, 2009; Sober and Sabes, 2005). According to this view, the brain simultaneously maintains gaze- and body-centered representations of the motor goal, effectively increasing flexibility and computational power. However, given inherent noise in coordinate transformations, the relative contribution of each of these reference frames to the output would be dependent on the available sensory cues. In the case of visual targets, the target and effector are initially coded in retinotopic and body-centered coordinates, respectively. Each of these "native" sensory sources would be converted to the "non-native" representation to define the motor goal simultaneously in gaze- and body-centered coordinates (Battaglia-Mayer et al., 2003; Buneo et al., 2002; Chang and Snyder, 2010; Medendorp et al., 2005; Pesaran et al., 2006), a view largely compatible with the present data. In contrast, in the case of unseen proprioceptive targets, both the target and effector are initially coded in body-centered space in higher-order somatosensory areas (Lacquaniti et al., 1995). In this case, optimal use

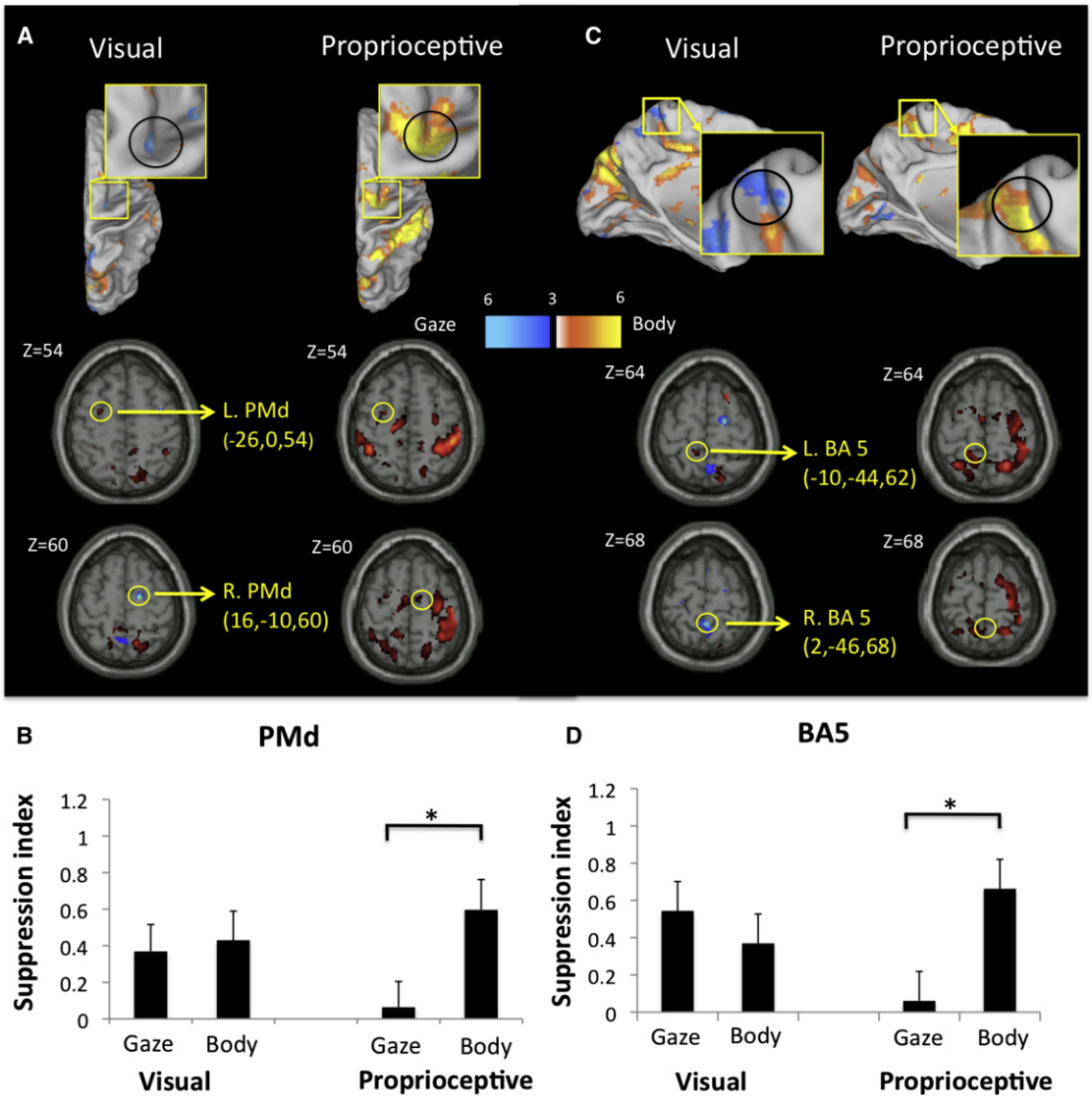

Figure 5. Change in Sensitivity to Gaze and Body as a Function of Target Modality in the PMd and BA 5

(A) Top: dorsal view of the right hemisphere with RS for gaze (in blue) and body (in red), showing the approximate location of the ROI in the PMd (circled in insets). Bottom: same activations overlaid on axial anatomical slices (ROIs circled).

(B) Suppression index for gaze and body in the visual and proprioceptive target conditions for PMd (data collapsed across both hemispheres).

(C) Top: medial view of the left hemisphere with RS for gaze (in blue) and body (in red), showing the approximate location of the ROI in the BA 5 (circled in insets). Bottom: same activations overlaid on axial anatomical slices (ROIs circled).

(D) Suppression index for gaze and body in the visual and proprioceptive target conditions for BA 5 (data collapsed across both hemispheres). Error bars represent SE. *$p < 0.05$.

of the available sensory information would be to attribute a greater weight to an intrinsic representation of the motor goal and to minimize the (noisy) process of deriving a visual representation of the motor goal from proprioceptive signals (McGuire and Sabes, 2009; Medendorp et al., 2005). In this framework, the present results provide neuroanatomical evidence for a multiplicity of reference frames for reaching whose relative contribution to the output is contingent upon the sensory modality of the target.

One of the most intriguing findings of the present study pertains to the reversal in sensitivity to gaze and body observed in the anterior precuneus for the two target modalities. It has been suggested that the human precuneus may constitute the human homolog of the monkey PRR (Connolly et al., 2003), because planning-related activity in this region is specific to arm-reaching movements (Astafiev et al., 2003; Connolly et al., 2003; Filimon et al., 2009; Tosoni et al., 2008) and shows contralateral topography with respect to the retinal coordinates of remembered visual targets (Fernandez-Ruiz et al., 2007). The present evidence for selective gaze-centered encoding of visual targets in the anterior precuneus is compatible with these views, supporting the

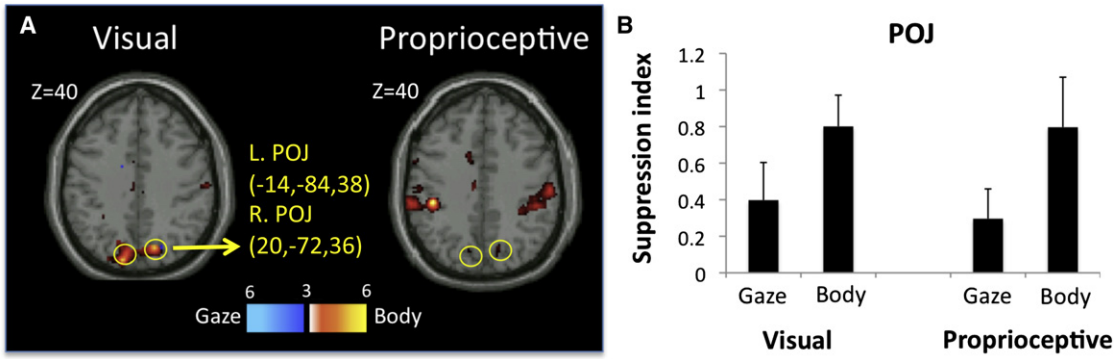

Figure 6. Mixed Sensitivity to Gaze and Body in the POJ

(A) Areas showing significant RS for gaze (in blue) and body (in red) in the visual and proprioceptive target conditions in the POJ (ROIs circled).

(B) Suppression index in the POJ (data collapsed across both hemispheres). Error bars represent SE.

notion that this area may be functionally related to the monkey PRR. In contrast, the strong body-centered encoding of proprioceptive targets observed in the same region of cortex is particularly striking, because it has long been argued that reach planning would be simplified by remapping all incoming sensory input into a common gaze-centered representation in the PPC (Cohen and Andersen, 2002; Medendorp et al., 2005). The present results thus suggest that there exists no rigid assignment of coordinate frames in the associative regions of the parietofrontal network, even in the dorsomedial PPC. Although single-cell evidence for body-centered encoding of proprioceptive targets in the monkey PRR still awaits, current knowledge suggests that such a scheme is possible. Indeed, area PEc in the monkey receives extensive projections from somatotopically-organized BA 5 and PMd (Bakola et al., 2010). As a result, it contains neurons that are modulated by passive and active upper limb movements (Breveglieri et al., 2006), many of which represent target locations in body-centered space using a receptive field code (Chang and Snyder, 2010). In this light, it may be more parsimonious to consider the dorsomedial PPC as containing neuronal populations capable of flexibly representing the motor goal using a gaze-centered, mixed, or body-centered reference frame according to the available inputs (Battaglia-Mayer et al., 2003; Chang and Snyder, 2010; McGuire and Sabes, 2009).

A critical issue relates to whether the reversal in sensitivity occurred within individual neurons or within separate spatially contiguous neuronal populations each using a fixed frame of reference. The former possibility is supported by both electrophysiological and computational work. Indeed, a significant proportion of cells in the monkey parietofrontal network, including PMd (Batista et al., 2007) and MIP (Chang and Snyder, 2010; Mullette-Gillman et al., 2009), show partially shifting receptive fields, which is indicative of a hybrid form of spatial encoding in which multiple reference frames are expressed (Pouget et al., 2002a). Computational models have proposed that a mixed representation may be accounted for by considering the PPC as an intermediate layer that uses basis functions to perform multidirectional coordinate transformations (Pouget and Snyder, 2000). Basis function units provide an efficient means of integrating the target-related sensory signals with the necessary postural signals (e.g., eye position, arm position) in order to define the motor goal. The appeal of the basis functions approach is that it allows single cells to simultaneously contribute to defining spatial positions in multiple frames of reference. Networks with such combinatorial properties also show optimal Bayesian statistical inference, with possible dynamic adjustment of the synaptic weight of each input according to context (Deneve et al., 2001). In this light, the sensory inputs to the PPC, either visual or proprioceptive, may have biased the representation expressed within single neurons toward a gaze- or body-centered mode of coding, leading to the observed reversal in representation. An alternative hypothesis is that the PPC encodes multiple reference frames by virtue of having distinct spatially segregated visuomotor and proprioceptivomotor neuronal populations (Filimon et al., 2009), each using a fixed gaze- or body-centered mode of representation, respectively. Obviously, the BOLD signal, while being ideally suited to capture the dominant frame of reference at the population level, cannot disentangle between these two possibilities.

Interestingly, we found a considerable difference in the mode of representation expressed in the POJ as compared to the anterior precuneus. Unlike the visual representation used in the anterior precuneus, the POJ encoded visual targets using a mixed representation, with a bias toward an intrinsic encoding of the motor goal (see Beurze et al., 2010 for similar observation). A mixed representation in the POJ supports recent electrophysiological work showing that a majority of cells in POJ's putative monkey homolog, area V6A (Galletti et al., 1999), encode the direction of movements using both retinocentric and spatial reference frames (Galletti et al., 1993; Marzocchi et al., 2008). Interestingly, many cells in monkey V6A are modulated by wrist orientation during reach-to-grasp movements (Fattori et al., 2010), consistent with the significant rotation at the wrist incurred by the present task. The fact that the frame of reference used in this area was relatively constant across the two target conditions is also in keeping with growing evidence suggesting that this region is active during the preparation of arm movements (Fattori et al., 2001), irrespective of whether targets are visually defined or not (Fattori et al., 2005). In humans, this region (i.e., superior parieto-occipital cortex) is more strongly activated during

passive viewing of tools when they are within graspable range (Gallivan et al., 2009). This affordance-like signal in POJ, being dependent upon the position of a target object with respect to the hand, is strongly compatible with the body-centered encoding observed here.

The different mixture of gaze- and body-centered reference frames observed here between the anterior precuneus and the POJ suggests some level of segregation within the reach-related regions of the human PPC. This is consistent with recent reports emphasizing functional subdivisions within these areas. For instance, the POJ, but not the anterior precuneus, shows more activity during on-line reaching when the effector is visible than when it is not (Filimon et al., 2009). Similarly, the POJ is specifically recruited for reaches to peripheral visual targets as compared to foveal targets, whereas more anterior regions of the SPL (peaking in mIPS) are activated independently of this parameter (Prado et al., 2005). Interestingly, a recent series of studies have provided human evidence for cytoarchitectonic delineation between the SPL/precuneus (7A, 7P) and the POJ (7M) (Scheperjans et al., 2008a; Scheperjans et al., 2008b; Scheperjans et al., 2005), which perhaps constitutes the anatomical underpinning of these functional distinctions.

One potential caveat relates to spatial attention, which is also thought to engage the anterior precuneus (Astafiev et al., 2003). Here we did not include an explicit attentional instruction in the static task, so as not to influence the nature of processing in the PPC. Still, we believe that attention is unlikely to account for the present results, because it would be counterbalanced across target modalities. Given that the visual and proprioceptive targets occupied the same spatial positions, orienting of attention should have produced similar activations, not a reversal in the mode of representation, as we observed across target modalities. Another methodological limitation relates to the impossibility, with the current design, to differentiate between anchor points for body-centered representations, because hand-, shoulder-, or head-centered coordinate systems would be undistinguishable from each other. This may account for the proportionally greater set of areas that showed repetition suppression for body than for gaze, because they may comprise neurons encoding the reach plan with respect to these multiple anchor points. Finally, caution should be exercised when drawing functional homologies between human and monkey data, because the BOLD signal reflects summed activity across many synaptic inputs to a region, whereas single-cell recordings reflect the output of single neurons (Logothetis et al., 2001). Nevertheless, the coordinate representations observed here in the dorsomedial PPC and premotor areas for visual targets are highly consistent with those reported in the monkey literature, suggesting good agreement between the two methodologies under these conditions.

Much emphasis is currently being devoted to developing neural prosthetics to decode movement goals through single-cell recordings in monkey PPC (Musallam et al., 2004). A holistic understanding of these neural mechanisms will require careful characterization of the task-related constraints that influence the frame of reference in which movement is encoded in this area. It also appears imperative to develop noninvasive means to reliably record these neural signals in the human brain if such technology is to be of widespread appeal. The present study provides a new means for assessing coordinate reference frames for action in humans and, in doing so, bridges a critical gap between monkey and human physiology.

EXPERIMENTAL PROCEDURES

Subjects

Eighteen right-handed subjects (8 males, age range 19–25) participated in the experiment. All gave informed written consent in accordance with the guidelines from the Human Subjects Committee, Office of Research, University of California, Santa Barbara. All subjects had normal vision and no history of neurological disease or psychiatric disorders. They were paid for their participation in the study.

Behavioral Validation

Prior to the fMRI experiment, all subjects came to the lab to practice the task outside the scanner and familiarize themselves with the sequence of stimuli (48 trials for each target modality). The setup and lighting conditions were identical to those inside the scanner, with subjects laying supine and doing the task while looking at the targets through a set of mirrors. Kinematic (Optotrak, Northern Digital) and eye tracking (IView, SensoMotoric Instruments) measurements confirmed that subjects promptly and accurately reached to the appropriate targets while maintaining gaze on the fixation lights. By the end of the practice session, all subjects reported great ease in completing the task accurately.

Apparatus

Subjects were positioned in the scanner with their head and neck padded with foam to prevent motion. They wore a set of headphones for ear protection and to hear the auditory stimuli. Visual stimuli were presented on a custom-built board made of thin opaque fiberglass that rested on subjects' abdomens, so as to be approximately perpendicular to the direction of gaze when looking through the mirrors (distance of board w/r to the eyes ~35 cm). Subjects were strapped to the table at the level of the chest to prevent excessive movement. The reaches were done in total darkness; hence, subjects could not see their reaching hand at any point.

The visual targets and the fixation lights consisted of fiber optic endings mounted on the board. A green central fixation light was positioned at the center of the board (0° with respect to subjects' body midline). In the visual condition, subjects reached with their right index finger toward one of two red visual targets that was positioned 5 cm above the central fixation light, either −5 cm to its left or +5 cm to its right (see Figure 1A). Subjects' left hands rested to the left of the board in the visual condition. In the proprioceptive condition, subjects reached with their right index finger toward the felt position of their unseen left thumb (left target) and index fingertip (right target), which were taped behind the board. Importantly, the fingertips occupied the same spatial position as the visual targets (turned off in the proprioceptive condition); therefore, the actual movement was identical for the two target modalities. In this arrangement, the targets could thus be defined as being either left or right in body-centered coordinates. Four orange peripheral fixation lights were positioned 6 cm above the central fixation light, either −15 and −5 cm to its left or +5 and +15 cm to its right. We manipulated where subjects were gazing during the reaches. When reaching to the left target, subjects were fixating on either the −15 or the +5 cm peripheral fixation lights (see Figure 1B). When reaching to the right target, subjects were fixating on either the −5 or the +15 cm peripheral fixation lights. Therefore, reaches were always performed in the peripheral visual field, with targets being defined either as left or right in gaze-centered coordinates. The visual angle subtended by the targets was ~8°. In sum, all trials fell evenly into a 2 body-centered target position (left, right) × 2 gaze-centered target position (left, right) factorial design (Figure 1B). An MR compatible button box was installed two centimeters below the central fixation light and served as the starting position.

Task Procedures

The two target conditions were performed in separate sessions a day apart, with their ordering pseudorandomized across subjects. Each of the two sessions comprised eight runs. In four of those runs, subjects performed the reaching movements (reach task), and in the remaining four runs, subjects were submitted to the same sequence of stimuli, with the only exception that they did not perform the reaching movements (static task). The amplitude of the reaches was short (~10 cm) so that they could be accomplished mostly through motion at the wrist, thereby minimizing motion of the upper arm. Yet subjects physically displaced their hand to touch the targets, justifying our use of the term "reaching" instead of "pointing" (i.e., angling the finger in the direction of the target without touching it; Culham et al., 2006).

We used a rapid single event-related design (see Figure 1C). Before each (reach) trial, subjects were required to press the button box. If subjects failed to press the button, the trial would not start, allowing us to keep some control over the flow of the experiment. The central fixation light was then lit, and subjects gazed at it for a period of 2, 4, 6, or 8 s, jittered to optimize the efficiency of the general linear model (GLM). After this delay, one of the four peripheral fixation lights was lit, and subjects directed their gaze to it. After a fixed 2 s delay, an auditory tone served as the go signal and prompted subjects to initiate the reach. The intensity of the tone (high or low pitch) signaled which target to reach to (left or right target). This arbitrary mapping was fixed for the entire experiment for each subject but was counterbalanced across subjects. Following the tone, subjects had a 2 s time window to execute the reach swiftly and accurately while maintaining fixation on the peripheral fixation light. After this delay, the central fixation light turned on again, prompting subjects to bring their right index finger back to the button box for the next trial. It should be noted that both visual targets remained lit for the entire duration of a trial in the visual condition. This was done to equate the two target conditions, because in the proprioceptive condition, somatosensory feedback of both fingertips was also present throughout each trial. In the static task, the same sequence of events took place (saccade to peripheral fixation light, auditory tone), but no reaching was performed. During this task, subjects were asked to remain attentive and alert to the sequence of stimuli but to not internally simulate the planning of a movement.

Each functional run comprised 48 trials, for a total of 196 reach trials and 196 static trials in each target condition (396 s/run). These were divided equally into each of the four target-gaze arrangements according to the 2 gaze × 2 body factorial design described previously (see Figure 1B). In addition to the 196 reach trials, 24 catch trials were randomly introduced into the trial sequence for each target condition. In these trials, the target cued by the auditory stimulus was not the one normally associated with the peripheral fixation light that was gazed at. The catch trials were added to introduce uncertainty as to the target of an upcoming reach and thus prevent subjects from planning a movement before the auditory cue. Given the limited number of catch trials, they were not analyzed further. The sequence of presentation of the trials was pseudorandomized such that we could assess the suppression in BOLD response associated with repetitions of either the gaze-centered target position or the body-centered target position. This was done by ensuring that each of these factors could be novel or repeated in consecutive trials, according to a one-back repetition suppression design (see Figure 1D) (Hamilton and Grafton, 2006). This gave 98 trials in which the gaze-centered target position was novel and 98 trials in which it was repeated; same for the body-centered target position. We ensured that these repetition effects were equally distributed across each target-gaze arrangement of the 2 gaze × 2 body factorial design and that each level (left, right) of the two factors was preceded and followed by every other type of trial equally often. The orthogonality of the design matrices was assessed prior to data collection to ensure adequate power to detect BOLD activations for all conditions of interest.

MRI Scanning and Analyses

Functional MRI recordings were conducted using a Siemens 3T Magnetom TIM Trio system with a 12 channel phased-array head coil. For each functional run, a T2-weighted echo planar gradient-echo imaging sequence sensitive to BOLD contrast was acquired (repetition time [TR] = 2000 ms; echo time [TE] = 30 ms; fractional anisotropy [FA] = 90°; field of view [FOV] = 192 mm). Each volume consisted of 37 slices acquired parallel to the anterior commissure-posterior commissure plane (interleaved acquisition; 3 mm with 0.5 mm gap; 3 × 3 mm in-plane resolution). Before the functional runs, a high-resolution T1-weighted sagittal sequence image of the whole brain was acquired (TR = 15 ms; TE = 4.2 ms; FA = 9°; FOV = 256 mm).

Functional MRI data preprocessing and statistical analyses were carried out in SPM5 (http://www.fil.ion.ucl.ac.uk/spm). The first three functional volumes of each run were removed to eliminate nonequilibrium effects of magnetization. Individual scans were spatially realigned to the middle image of the time series, slice-time corrected, registered to the anatomical image, and normalized to MNI space (resampled at 3 × 3 × 3 mm resolution). Images were temporally high-pass filtered with a 128 s cutoff. The functional data were then smoothed with an 8 mm full-width half-maximum isotropic Gaussian kernel. Finally, even with the head perfectly stable, the dislocation of a mass near but outside of the head coil can induce signal changes in the images. We thus utilized a weighted least-squares algorithm to inversely weigh each image by the inverse of its variance, therefore minimizing the impact of these images in the estimation of the GLM (Diedrichsen and Shadmehr, 2005).

First-level fMRI analyses, estimated for each subject individually, were performed according to the GLM. These analyses addressed two aims. The first aim was to identify reach-related regions for each target modality and discard extraneous activities associated with eye movements and auditory stimulation. This was done by comparing the reach trials to the static trials separately for each target modality. The second aim was to assess the suppression in the BOLD response associated with repetitions of either the gaze-centered or the body-centered target positions. Only the reach trials were considered in this analysis. Each trial was modeled as a 2 s boxcar between the appearance of the peripheral fixation light and the auditory cue. It was convolved with the standard gamma-shaped hemodynamic response function and temporal derivative provided by SPM5.

In the first analysis, the fMRI time series was fitted with eight regressors (and their temporal derivatives) corresponding to the four target-gaze arrangements (Figure 1B) for each of the two tasks (reach, static), plus a regressor of noninterest for the catch trials. Reach-related activations were obtained by compound linear contrasts between the parameter estimates for reach and for static, including the temporal derivatives (reach > static). In the second analysis, the fMRI time series was fitted with 16 regressors (and their temporal derivatives) corresponding to the four target-gaze arrangements (Figure 1B), the factors of which were either novel or repeated (NovelGaze-NovelBody, NovelGaze-RepeatedBody, RepeatedGaze-NovelBody, RepeatedGaze-RepeatedBody), plus a regressor of noninterest for the catch trials. RS for gaze was assessed by compound linear contrasts between the parameter estimates in which gaze was novel and in which gaze was repeated, including the temporal derivatives (NovelGaze > RepeatedGaze). The same was done to assess RS for body (NovelBody > RepeatedBody).

Second-level random-effects analyses were then applied to individual contrasts of parameter estimates to obtain a population estimate. The reach-related activation maps (set at $p < 0.001$ uncorrected for multiple comparisons) were used as inclusive masks for subsequent analyses of RS. Significant RS effects surviving a voxel-level threshold of $p < 0.005$ uncorrected and minimum cluster size of 10 voxels are reported. Given the a priori prediction that task and RS effects would be localized in parietofrontal areas, this threshold was considered sufficient to adjust for multiple test comparisons. We confirmed that the reciprocal contrasts (repeated > novel) did not yield significant activity in any of the reach-related regions ($p < 0.005$).

For visualization purposes, the t images were mapped to the partially inflated cortical surface of the population average landmark and surface-based (PALS-B12) atlas (Van Essen, 2005) using the Caret software application. The PALS-B12 atlas represents the surface registration of 12 normal adult high-resolution scans, which can be used as an unbiased template for displaying images from group fMRI analyses. Parcellation of SPL microanatomical areas from peak MNI coordinates was based on probabilistic maps derived from multimodal analysis of cyto- and receptoarchitecture in postmortem human brains (Scheperjans et al., 2008a; Scheperjans et al., 2008b; Scheperjans et al., 2005).

An ROI approach was used to quantify the relative RS for gaze and body with MarsBar (http://marsbar.sourceforge.net/). ROIs were defined as 8 mm

spheres around the peak of every region showing significant RS for gaze or body in the visual condition (listed in Table 1). They comprised, in an anteroposterior direction: bilateral PMd, bilateral PMv, right postcentral sulcus (BA 2), bilateral paracentral lobule (BA 5), bilateral aIPS, bilateral mIPS, bilateral anterior precuneus, and bilateral POJ (MFG was not included). The sensitivity to gaze and body was then assessed at these same coordinates for both the visual and proprioceptive conditions. To do so, we calculated a suppression index (i.e., the difference in mean parameter estimates between novel and repeated trials). These were calculated independently for gaze and body, as well as for each target modality. The suppression indexes for each subject were submitted to a two-way repeated-measures ANOVA with factors of sensitivity (gaze, body) and target modality (visual, proprioceptive). Significant interactions were broken down with paired t tests ($p < 0.05$).

SUPPLEMENTAL INFORMATION

Supplemental Information includes three figures and two tables and can be found online at doi:10.1016/j.neuron.2010.11.002.

ACKNOWLEDGMENTS

We thank Mario Mendoza for MRI technical assistance and Fabrice Sarlegna for helpful comments. This work was supported by a postdoctoral fellowship awarded by the Fyssen Foundation to P.-M.B., by Public Health Service grant NS44393, and by the Institute for Collaborative Biotechnologies through contract W911NF- 09-D-0001 from the U.S. Army Research Office.

Accepted: September 7, 2010
Published: November 17, 2010

REFERENCES

Andersen, R.A., and Buneo, C.A. (2002). Intentional maps in posterior parietal cortex. Annu. Rev. Neurosci. *25*, 189–220.

Astafiev, S.V., Shulman, G.L., Stanley, C.M., Snyder, A.Z., Van Essen, D.C., and Corbetta, M. (2003). Functional organization of human intraparietal and frontal cortex for attending, looking, and pointing. J. Neurosci. *23*, 4689–4699.

Bakola, S., Gamberini, M., Passarelli, L., Fattori, P., and Galletti, C. (2010). Cortical connections of parietal field PEc in the macaque: Linking vision and somatic sensation for the control of limb action. Cereb. Cortex *20*, 2592–2604.

Batista, A.P., Buneo, C.A., Snyder, L.H., and Andersen, R.A. (1999). Reach plans in eye-centered coordinates. Science *285*, 257–260.

Batista, A.P., Santhanam, G., Yu, B.M., Ryu, S.I., Afshar, A., and Shenoy, K.V. (2007). Reference frames for reach planning in macaque dorsal premotor cortex. J. Neurophysiol. *98*, 966–983.

Battaglia-Mayer, A., Caminiti, R., Lacquaniti, F., and Zago, M. (2003). Multiple levels of representation of reaching in the parieto-frontal network. Cereb. Cortex *13*, 1009–1022.

Beurze, S.M., Toni, I., Pisella, L., and Medendorp, W.P. (2010). Reference frames for reach planning in human parietofrontal cortex. J. Neurophysiol. *104*, 1736–1745.

Breveglieri, R., Galletti, C., Gamberini, M., Passarelli, L., and Fattori, P. (2006). Somatosensory cells in area PEc of macaque posterior parietal cortex. J. Neurosci. *26*, 3679–3684.

Buneo, C.A., Jarvis, M.R., Batista, A.P., and Andersen, R.A. (2002). Direct visuomotor transformations for reaching. Nature *416*, 632–636.

Chang, S.W., and Snyder, L.H. (2010). Idiosyncratic and systematic aspects of spatial representations in the macaque parietal cortex. Proc. Natl. Acad. Sci. USA *107*, 7951–7956.

Cohen, Y.E., and Andersen, R.A. (2000). Reaches to sounds encoded in an eye-centered reference frame. Neuron *27*, 647–652.

Cohen, Y.E., and Andersen, R.A. (2002). A common reference frame for movement plans in the posterior parietal cortex. Nat. Rev. Neurosci. *3*, 553–562.

Connolly, J.D., Andersen, R.A., and Goodale, M.A. (2003). FMRI evidence for a 'parietal reach region' in the human brain. Exp. Brain Res. *153*, 140–145.

Culham, J.C., Cavina-Pratesi, C., and Singhal, A. (2006). The role of parietal cortex in visuomotor control: What have we learned from neuroimaging? Neuropsychologia *44*, 2668–2684.

Deneve, S., Latham, P.E., and Pouget, A. (2001). Efficient computation and cue integration with noisy population codes. Nat. Neurosci. *4*, 826–831.

Desimone, R. (1996). Neural mechanisms for visual memory and their role in attention. Proc. Natl. Acad. Sci. USA *93*, 13494–13499.

Diedrichsen, J., and Shadmehr, R. (2005). Detecting and adjusting for artifacts in fMRI time series data. Neuroimage *27*, 624–634.

Fattori, P., Gamberini, M., Kutz, D.F., and Galletti, C. (2001). 'Arm-reaching' neurons in the parietal area V6A of the macaque monkey. Eur. J. Neurosci. *13*, 2309–2313.

Fattori, P., Kutz, D.F., Breveglieri, R., Marzocchi, N., and Galletti, C. (2005). Spatial tuning of reaching activity in the medial parieto-occipital cortex (area V6A) of macaque monkey. Eur. J. Neurosci. *22*, 956–972.

Fattori, P., Raos, V., Breveglieri, R., Bosco, A., Marzocchi, N., and Galletti, C. (2010). The dorsomedial pathway is not just for reaching: Grasping neurons in the medial parieto-occipital cortex of the macaque monkey. J. Neurosci. *30*, 342–349.

Fernandez-Ruiz, J., Goltz, H.C., DeSouza, J.F., Vilis, T., and Crawford, J.D. (2007). Human parietal "reach region" primarily encodes intrinsic visual direction, not extrinsic movement direction, in a visual motor dissociation task. Cereb. Cortex *17*, 2283–2292.

Filimon, F., Nelson, J.D., Huang, R.S., and Sereno, M.I. (2009). Multiple parietal reach regions in humans: Cortical representations for visual and proprioceptive feedback during on-line reaching. J. Neurosci. *29*, 2961–2971.

Galletti, C., Battaglini, P.P., and Fattori, P. (1993). Parietal neurons encoding spatial locations in craniotopic coordinates. Exp Brain Res *96*, 221–229.

Galletti, C., Fattori, P., Kutz, D.F., and Battaglini, P.P. (1997). Arm movement-related neurons in the visual area V6A of the macaque superior parietal lobule. Eur. J. Neurosci. *9*, 410–413.

Galletti, C., Fattori, P., Kutz, D.F., and Gamberini, M. (1999). Brain location and visual topography of cortical area V6A in the macaque monkey. Eur. J. Neurosci. *11*, 575–582.

Gallivan, J.P., Cavina-Pratesi, C., and Culham, J.C. (2009). Is that within reach? fMRI reveals that the human superior parieto-occipital cortex encodes objects reachable by the hand. J. Neurosci. *29*, 4381–4391.

Grafton, S.T., Mazziotta, J.C., Woods, R.P., and Phelps, M.E. (1992). Human functional anatomy of visually guided finger movements. Brain *115*, 565–587.

Graziano, M.S., and Gross, C.G. (1998). Spatial maps for the control of movement. Curr. Opin. Neurobiol. *8*, 195–201.

Graziano, M.S., Yap, G.S., and Gross, C.G. (1994). Coding of visual space by premotor neurons. Science *266*, 1054–1057.

Grefkes, C., and Fink, G.R. (2005). The functional organization of the intraparietal sulcus in humans and monkeys. J. Anat. *207*, 3–17.

Grill-Spector, K., Henson, R., and Martin, A. (2006). Repetition and the brain: Neural models of stimulus-specific effects. Trends Cogn. Sci. (Regul. Ed.) *10*, 14–23.

Hamilton, A.F., and Grafton, S.T. (2006). Goal representation in human anterior intraparietal sulcus. J. Neurosci. *26*, 1133–1137.

Jackson, S.R., Newport, R., Husain, M., Harvey, M., and Hindle, J.V. (2000). Reaching movements may reveal the distorted topography of spatial representations after neglect. Neuropsychologia *38*, 500–507.

Johnson, P.B., and Ferraina, S. (1996). Cortical networks for visual reaching: Intrinsic frontal lobe connectivity. Eur. J. Neurosci. *8*, 1358–1362.

Karnath, H.O., and Perenin, M.T. (2005). Cortical control of visually guided reaching: Evidence from patients with optic ataxia. Cereb. Cortex *15*, 1561–1569.

Khan, A.Z., Pisella, L., Vighetto, A., Cotton, F., Luauté, J., Boisson, D., Salemme, R., Crawford, J.D., and Rossetti, Y. (2005). Optic ataxia errors depend on remapped, not viewed, target location. Nat Neurosci *8*, 418–420.

Lacquaniti, F., Guigon, E., Bianchi, L., Ferraina, S., and Caminiti, R. (1995). Representing spatial information for limb movement: Role of area 5 in the monkey. Cereb. Cortex *5*, 391–409.

Levy, I., Schluppeck, D., Heeger, D.J., and Glimcher, P.W. (2007). Specificity of human cortical areas for reaches and saccades. J. Neurosci. *27*, 4687–4696.

Logothetis, N.K., Pauls, J., Augath, M., Trinath, T., and Oeltermann, A. (2001). Neurophysiological investigation of the basis of the fMRI signal. Nature *412*, 150–157.

Marzocchi, N., Breveglieri, R., Galletti, C., and Fattori, P. (2008). Reaching activity in parietal area V6A of macaque: Eye influence on arm activity or retinocentric coding of reaching movements? Eur. J. Neurosci. *27*, 775–789.

McGuire, L.M., and Sabes, P.N. (2009). Sensory transformations and the use of multiple reference frames for reach planning. Nat. Neurosci. *12*, 1056–1061.

Medendorp, W.P., Goltz, H.C., Vilis, T., and Crawford, J.D. (2003). Gaze-centered updating of visual space in human parietal cortex. J. Neurosci. *23*, 6209–6214.

Medendorp, W.P., Goltz, H.C., Crawford, J.D., and Vilis, T. (2005). Integration of target and effector information in human posterior parietal cortex for the planning of action. J. Neurophysiol. *93*, 954–962.

Medendorp, W.P., Beurze, S.M., Van Pelt, S., and Van Der Werf, J. (2008). Behavioral and cortical mechanisms for spatial coding and action planning. Cortex *44*, 587–597.

Mullette-Gillman, O.A., Cohen, Y.E., and Groh, J.M. (2009). Motor-related signals in the intraparietal cortex encode locations in a hybrid, rather than eye-centered reference frame. Cereb. Cortex *19*, 1761–1775.

Musallam, S., Corneil, B.D., Greger, B., Scherberger, H., and Andersen, R.A. (2004). Cognitive control signals for neural prosthetics. Science *305*, 258–262.

Pellijeff, A., Bonilha, L., Morgan, P.S., McKenzie, K., and Jackson, S.R. (2006). Parietal updating of limb posture: An event-related fMRI study. Neuropsychologia *44*, 2685–2690.

Pesaran, B., Nelson, M.J., and Andersen, R.A. (2006). Dorsal premotor neurons encode the relative position of the hand, eye, and goal during reach planning. Neuron *51*, 125–134.

Pouget, A., and Snyder, L.H. (2000). Computational approaches to sensorimotor transformations. Nat. Neurosci. Suppl. *3*, 1192–1198.

Pouget, A., Deneve, S., and Duhamel, J.R. (2002a). A computational perspective on the neural basis of multisensory spatial representations. Nat. Rev. Neurosci. *3*, 741–747.

Pouget, A., Ducom, J.C., Torri, J., and Bavelier, D. (2002b). Multisensory spatial representations in eye-centered coordinates for reaching. Cognition *83*, B1–B11.

Prado, J., Clavagnier, S., Otzenberger, H., Scheiber, C., Kennedy, H., and Perenin, M.T. (2005). Two cortical systems for reaching in central and peripheral vision. Neuron *48*, 849–858.

Rushworth, M.F., Nixon, P.D., and Passingham, R.E. (1997). Parietal cortex and movement. I. Movement selection and reaching. Exp. Brain Res. *117*, 292–310.

Scheperjans, F., Palomero-Gallagher, N., Grefkes, C., Schleicher, A., and Zilles, K. (2005). Transmitter receptors reveal segregation of cortical areas in the human superior parietal cortex: Relations to visual and somatosensory regions. Neuroimage *28*, 362–379.

Scheperjans, F., Eickhoff, S.B., Hömke, L., Mohlberg, H., Hermann, K., Amunts, K., and Zilles, K. (2008a). Probabilistic maps, morphometry, and variability of cytoarchitectonic areas in the human superior parietal cortex. Cereb. Cortex *18*, 2141–2157.

Scheperjans, F., Hermann, K., Eickhoff, S.B., Amunts, K., Schleicher, A., and Zilles, K. (2008b). Observer-independent cytoarchitectonic mapping of the human superior parietal cortex. Cereb. Cortex *18*, 846–867.

Sereno, M.I., Pitzalis, S., and Martinez, A. (2001). Mapping of contralateral space in retinotopic coordinates by a parietal cortical area in humans. Science *294*, 1350–1354.

Sirigu, A., Cohen, L., Duhamel, J.R., Pillon, B., Dubois, B., and Agid, Y. (1995). A selective impairment of hand posture for object utilization in apraxia. Cortex *31*, 41–55.

Snyder, L.H., Batista, A.P., and Andersen, R.A. (1997). Coding of intention in the posterior parietal cortex. Nature *386*, 167–170.

Sober, S.J., and Sabes, P.N. (2005). Flexible strategies for sensory integration during motor planning. Nat. Neurosci. *8*, 490–497.

Tosoni, A., Galati, G., Romani, G.L., and Corbetta, M. (2008). Sensory-motor mechanisms in human parietal cortex underlie arbitrary visual decisions. Nat. Neurosci. *11*, 1446–1453.

Van Essen, D.C. (2005). A Population-Average, Landmark- and Surface-based (PALS) atlas of human cerebral cortex. Neuroimage *28*, 635–662.

Van Pelt, S., Toni, I., Diedrichsen, J., and Medendorp, W.P. (2010). Repetition suppression dissociates spatial frames of reference in human saccade generation. J. Neurophysiol. *104*, 1239–1248.